Cell Reports, Volume *26*

Supplemental Information

Mammalian *Pum1* and *Pum2* Control Body Size via Translational Regulation of the Cell Cycle Inhibitor *Cdkn1b*

Kaibo Lin, Wenan Qiang, Mengyi Zhu, Yan Ding, Qinghua Shi, Xia Chen, Emese Zsiros, Kun Wang, Xiaodi Yang, Takeshi Kurita, and Eugene Yujun Xu

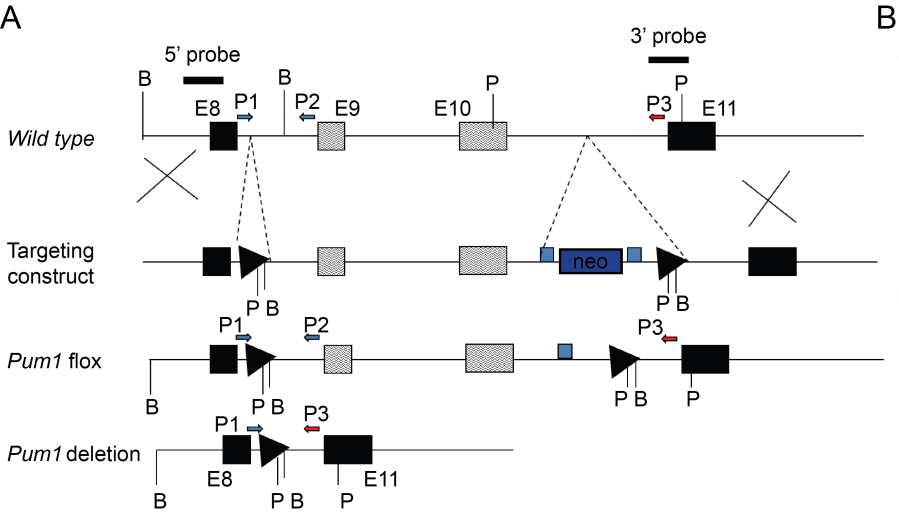

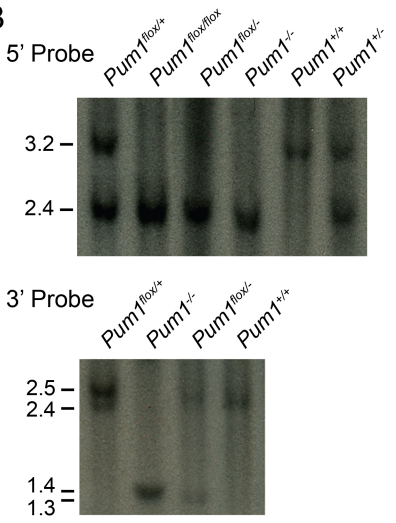

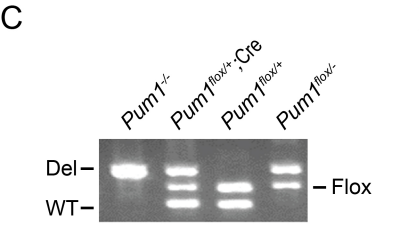

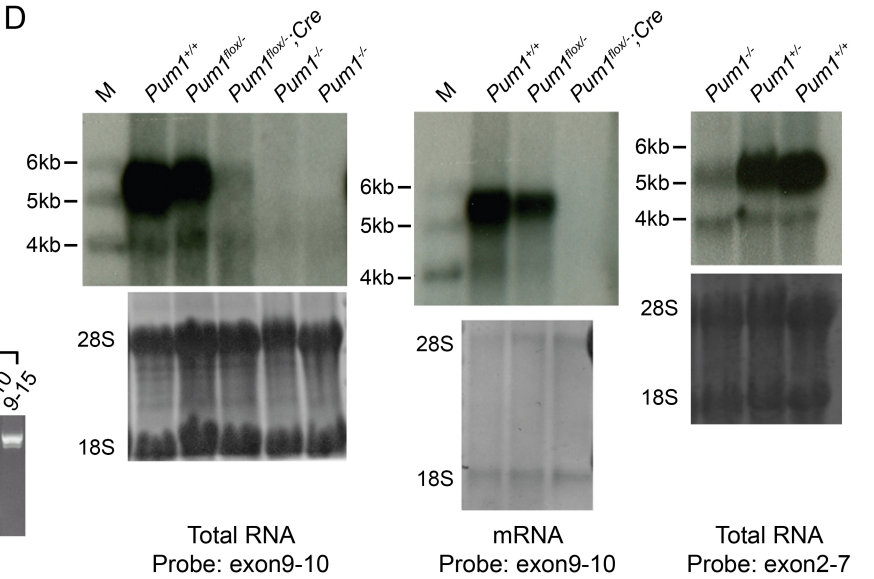

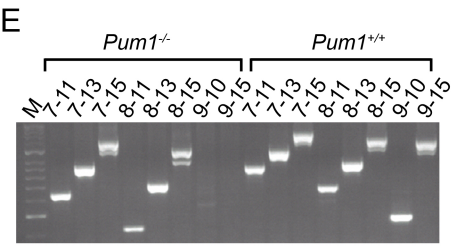

F

$Pum1^{flox/-}$ × $Pum1^{flox/-}$

Animals	$Pum1^{flox/flox}$	$Pum1^{flox/-}$	$Pum1^{-/-}$
Total(122)	44 (36.07%)	59 (48.36%)	19 (15.57%)**
Male(60)	22	29	9
Female(62)	22	30	10

Figure S1. Generation and validation of loss-of-function *Pum1* knockout allele, Related to Figure 1.

(A) Pum1 knockout strategy. Targeting construct, floxed allele and knockout allele are shown. B-BamHI, P-PstI, P1, P2 and P3 are primers designed for genotyping. Positions of probes used for Southern hybridization in (B) are indicated.

(B) Southern hybridization of various genotypes containing wildtype, floxed and knockout alleles produced fragments of predicted size and validated the gene targeting strategy.

(C) PCR genotyping distinguishes wildtype, floxed and knockout alleles. The three bands seen in *Pum1*$^{flox/-}$ mice results from leaky expression of Vasa-Cre in somatic tissue.

(D) Northern hybridization of testicular total RNA and mRNA using two different cDNA probes. A probe for Exon 9 and10 confirmed absence of full-length transcript in in *Pum1*$^{-/-}$ testes and highly reduced levels in Vasa-cre Pum1flox/- mice, with remaining signal likely resulting from expression in testicular somatic cells not subject to Vasa-Cre recombination. mRNA Northern using the same probe further demonstrated reduction of wild type transcripts in heterozygotes and absence of the transcripts in Vasa-cre *Pum1*$^{flox/-}$ testes. A probe spanning exon 2 to exon 7 detected very low levels of truncated transcripts containing exons 2 to 7.

(E) RT-PCR using primers detecting different exons of Pum1 confirmed the complete absence of full-length transcripts in *Pum1*$^{-/-}$ testes. Any remaining Pum1 transcripts detected lacked exons 9 and 10 based on size shift and confirmed by sequencing of the PCR products.

(F) Intercrossing of *Pum1*$^{+/-}$ mice produces fewer *Pum1*$^{-/-}$ pups than expected based on Mendelian ratios, suggesting loss of a small proportion of homozygotes before birth. ** $P<0.01$.

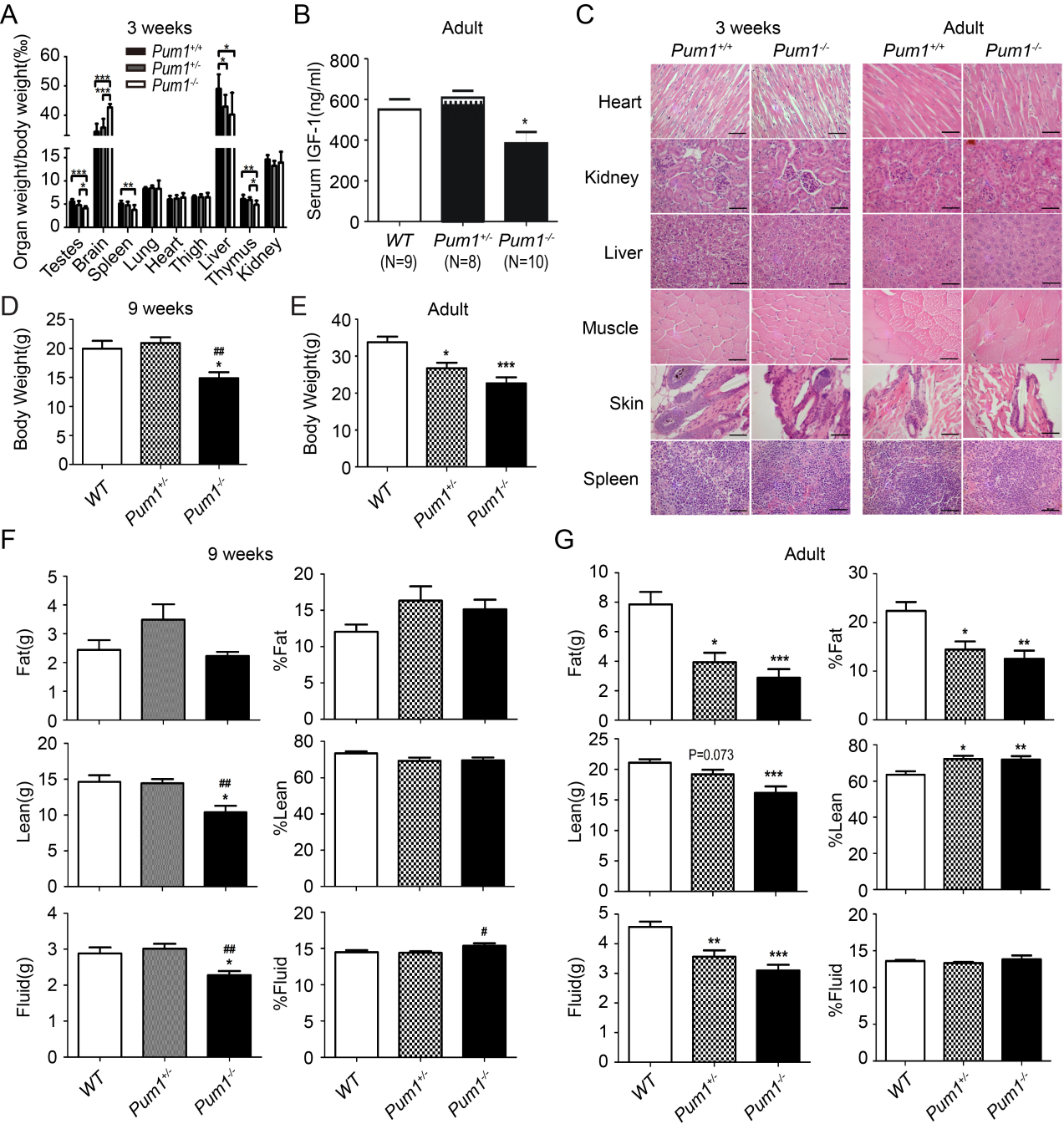
A
3 weeks
Pum1+/+
Pum1+/-
Pum1-/-
Organ weight/body weight(‰)
Testes
Brain
Spleen
Lung
Heart
Thigh
Liver
Thymus
Kidney
B
Adult
Serum IGF-1(ng/ml)
WT
(N=9)
Pum1+/-
(N=8)
Pum1-/-
(N=10)
C
3 weeks
Adult
Pum1+/+
Pum1-/-
Heart
Kidney
Liver
Muscle
Skin
Spleen
D
9 weeks
Body Weight(g)
WT
Pum1+/-
Pum1-/-
E
Adult
Body Weight(g)
F
9 weeks
Fat(g)
%Fat
Lean(g)
%Lean
Fluid(g)
%Fluid
G
Adult
P=0.073

Figure S2. Organ weight, organ/body ratio, serum IGF-1, organ histology and body composition from wild type and *Pum1* mutant mice, Related to Figure 2.

(A) Ratio of organ weight over body weight from 3wk old mice is similar between knockout mice and wild type littermates.

(B) Serum total IGF-1 level in 2-month-old Pum1$^{+/+}$*(n=12)*, *Pum1*$^{+/-}$ (n=8) and *Pum1*$^{-/-}$ (n=8) mice, measured by using active mouse/rat IGF-1 ELISA kit. IGF-1 level in *Pum1*$^{-/-}$ mice was significantly decreased (P<0.05) compared with those of *Pum1*$^{+/+}$ or *Pum1*$^{+/-}$ mice. Each value represents means ±S.E.M. *p<0.05 (Student's t-test).

(C) Histological analysis of a representative panel of organs harvested from 3-week-old and adult *Pum1*$^{+/+}$ and *Pum1*$^{-/-}$ mice. Sections were stained with hematoxylin/eosin. Scale bars, 200 μm.

(D and E) Body weight of 9-week-old (D) and adult (E) *WT*, *Pum1*$^{+/-}$ and *Pum1*$^{-/-}$ female mice.

(F and G) Body composition of 9-week-old(F) and adult(G) *WT*, *Pum1*$^{+/-}$ and *Pum1*$^{-/-}$ females (mass and percentage of fat, lean and fluid) were measured by NMR.

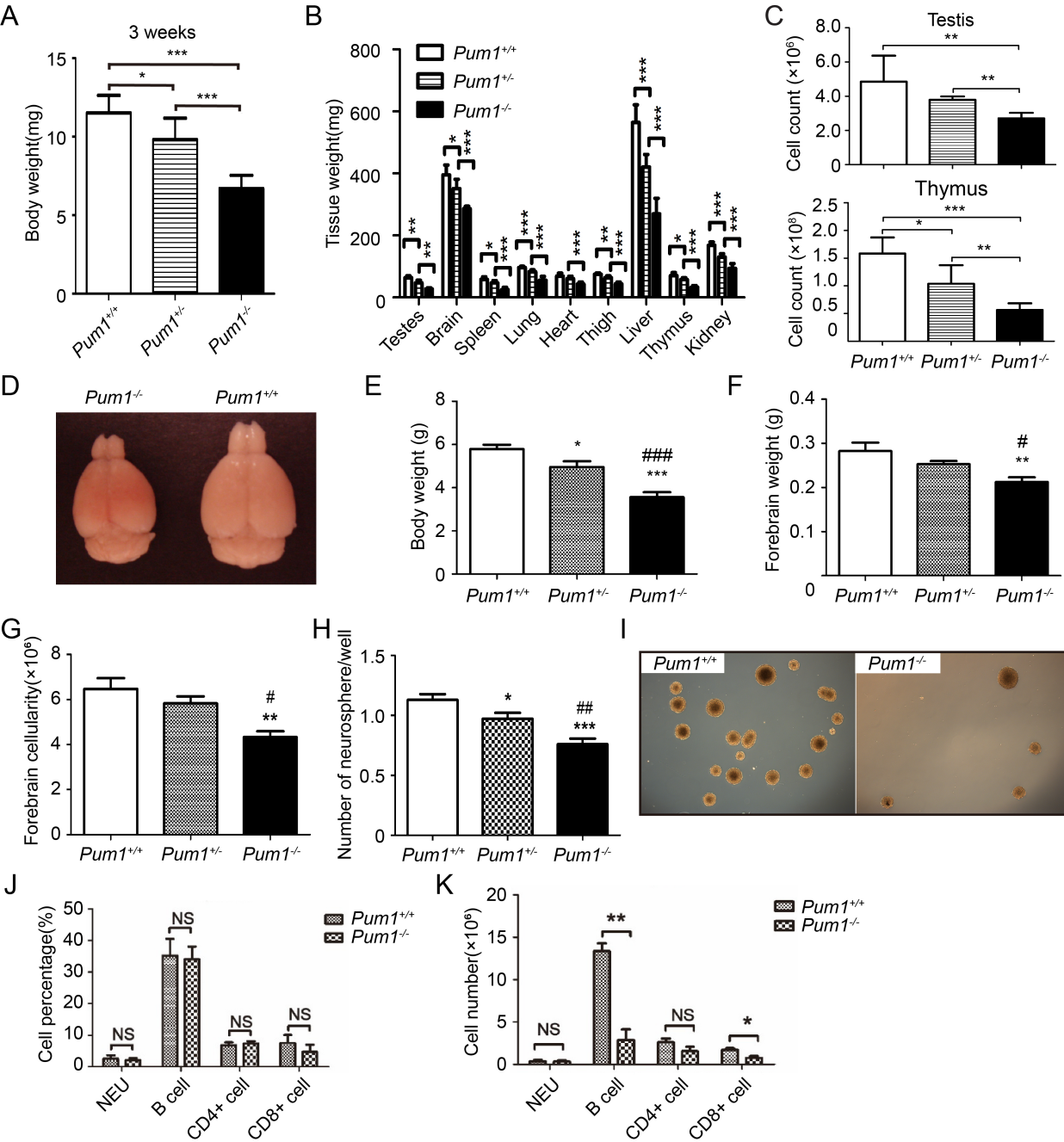
A
3 weeks
Body weight(mg)
Pum1+/+
Pum1+/-
Pum1-/-
B
Tissue weight(mg)
Testes
Brain
Spleen
Lung
Heart
Thigh
Liver
Thymus
Kidney
C
Testis
Cell count (×10^6)
Thymus
Cell count (×10^8)
D
Pum1-/-
Pum1+/+
E
Body weight (g)
F
Forebrain weight (g)
G
Forebrain cellularity(×10^6)
H
Number of neurosphere/well
I
J
Cell percentage(%)
NEU
B cell
CD4+ cell
CD8+ cell
K
Cell number(×10^6)

Figure S3. Reduced organ weight in Pum1 mutant mice and reduced cell proliferation rate of Pum1 mutant cells in neonatal brain and bone marrow contributing to reduced weight and cell number in forebrain and spleen, Related to Figure 2.

(A) Body weight of 3-week-old *WT*, *Pum1*$^{+/-}$ and *Pum1*$^{-/-}$ males.

(B) Organ weights of 3-week-old *WT*, *Pum1*$^{+/-}$ and *Pum1*$^{-/-}$ males.

(C) Total cell count of testis and thymus of 3-week-old *WT*, *Pum1*$^{+/-}$and *Pum1*$^{-/-}$ males.

(D) *Pum1* homozygotes mice exhibited a proportionally smaller brain including forebrain.

(E) Neonatal P7 *Pum1* homozygotes and heterozygotes are smaller than wildtype in body weight.

(F) P7 *Pum1* homozygotes are also significantly smaller than wildtype in forebrain weight while heterozygotes are smaller but not significantly.

(G) The total cell number in P7 *Pum1*$^{-/-}$ forebrain is significantly reduced.

(H and I) The number of neurospheres cultured from P7 Pum1 homozygote. Forebrain was reduced in number(H) and size(I) of neurospheres than those of wildtype.

(J) Flow cytometry analysis showed that the smaller spleen from Pum1 homozygotes contain all types of cells at the same proportion as those in wildtype.

(K) The absolute number of different cell types is significantly reduced for B cells, CD8+ T cells, but CD4+ T cells were reduced but not above significance level. The neutral (NEU) cells were not different. t-test: *, $p < 0.05$; **, $p < 0.01$; ***, $p<0.001$; NS, $P > 0.05$.

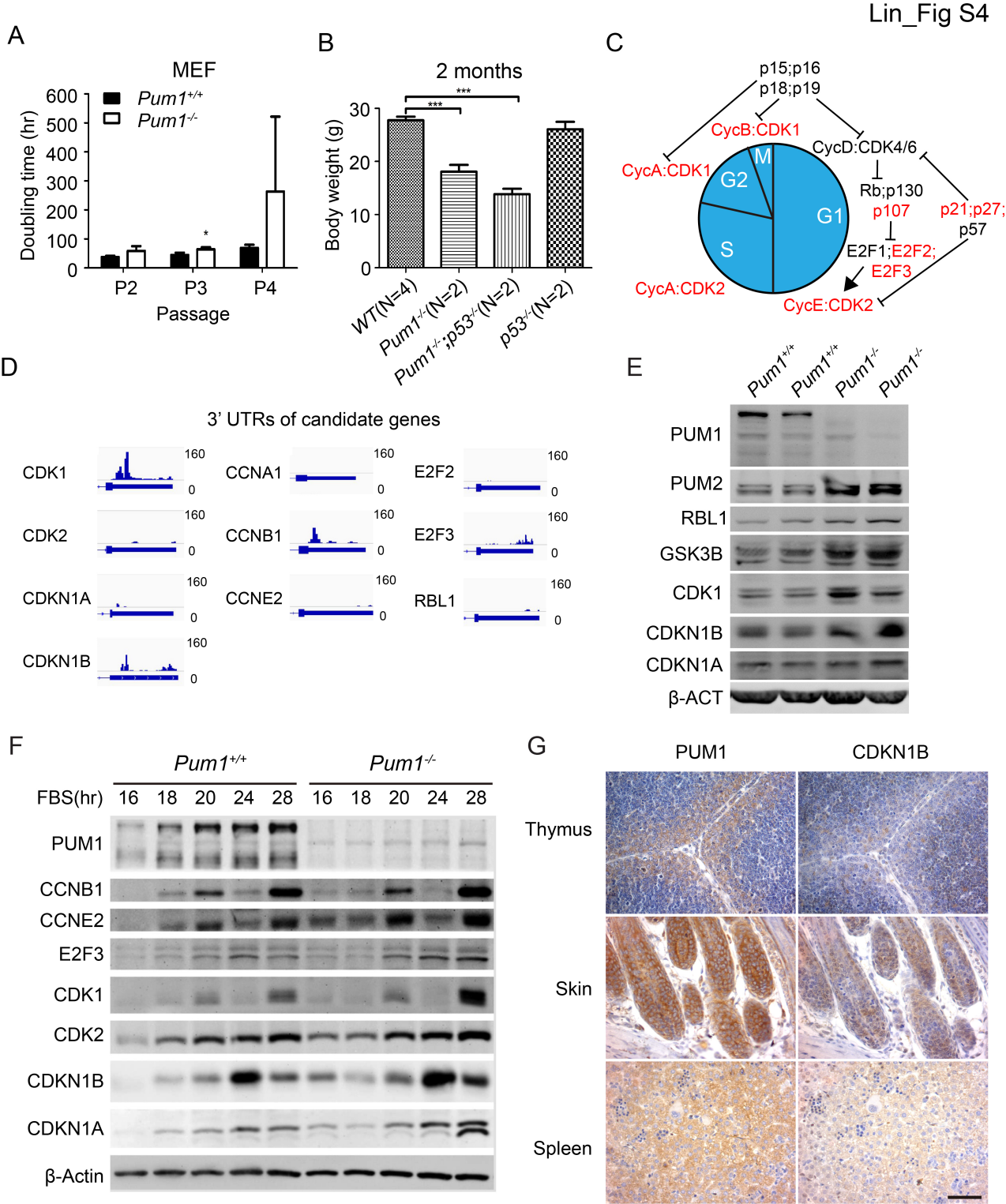
A
MEF
Pum1+/+
Pum1-/-
Doubling time (hr)
600
500
400
300
200
100
0
*
P2
P3
P4
Passage
B
2 months
***
***
Body weight (g)
30
20
10
0
WT(N=4)
Pum1-/-(N=2)
Pum1-/-;p53-/-(N=2)
p53-/-(N=2)
C
p15;p16
p18;p19
CycB:CDK1
CycD:CDK4/6
CycA:CDK1
M
G2
G1
S
Rb;p130
p107
p21;p27;
p57
E2F1;E2F2;
E2F3
CycA:CDK2
CycE:CDK2
D
3' UTRs of candidate genes
CDK1
CCNA1
E2F2
CDK2
CCNB1
E2F3
CDKN1A
CCNE2
RBL1
CDKN1B
160
0
E
Pum1+/+
Pum1+/+
Pum1-/-
Pum1-/-
PUM1
PUM2
RBL1
GSK3B
CDK1
CDKN1B
CDKN1A
β-ACT
F
Pum1+/+
Pum1-/-
FBS(hr)
16
18
20
24
28
16
18
20
24
28
PUM1
CCNB1
CCNE2
E2F3
CDK1
CDK2
CDKN1B
CDKN1A
β-Actin
G
PUM1
CDKN1B
Thymus
Skin
Spleen

Figure S4. Expression levels of *Pum1* and *Cdkn1b* in different tissues often exhibited opposite pattern, consistent with repression of Cdkn1b by Pum1 protein, Related to Figure 3.

(A) Doubling time of *Pum1*$^{+/+}$ and *Pum1*$^{-/-}$ MEF from passage 2 to passage 4.

(B) *Pum1*$^{-/-}$;*p53*$^{-/-}$ double mutant remained as small as *Pum1*$^{-/-}$ at 2-month old, excluding p53 upregulation as the main contributor towards body size reduction in *Pum1* mutants.

(C) Diagram shows that key regulators in cell cycle progression. Genes containing PBE in 3'UTR were highlighted in red.

(D) Peaks of read density tracks indicate regions of 3'UTR of cell cycle genes directly bound by human PUM2 in K562 cells (Van Nostrand et al., 2016).

(E) Protein expression of cell cycle regulators with PBEs in *Pum1* knockout and wild type MEFs.

(F) Protein expression profile of PUM1 and cell cycle genes in synchronized MEFs cells at different time points after re-feeding with FBS. Loss of PUM1 in MEF cells resulted in cell cycle-dependent increase in CDKN1B as well as CDK1, CycE2 etc.

(G) Immunostaining of consecutive tissue sections from wild type neonatal mice (8dpp). Cells with high PUM1 protein signals often exhibit low CDKN1b signal. Scale bar=50μm.

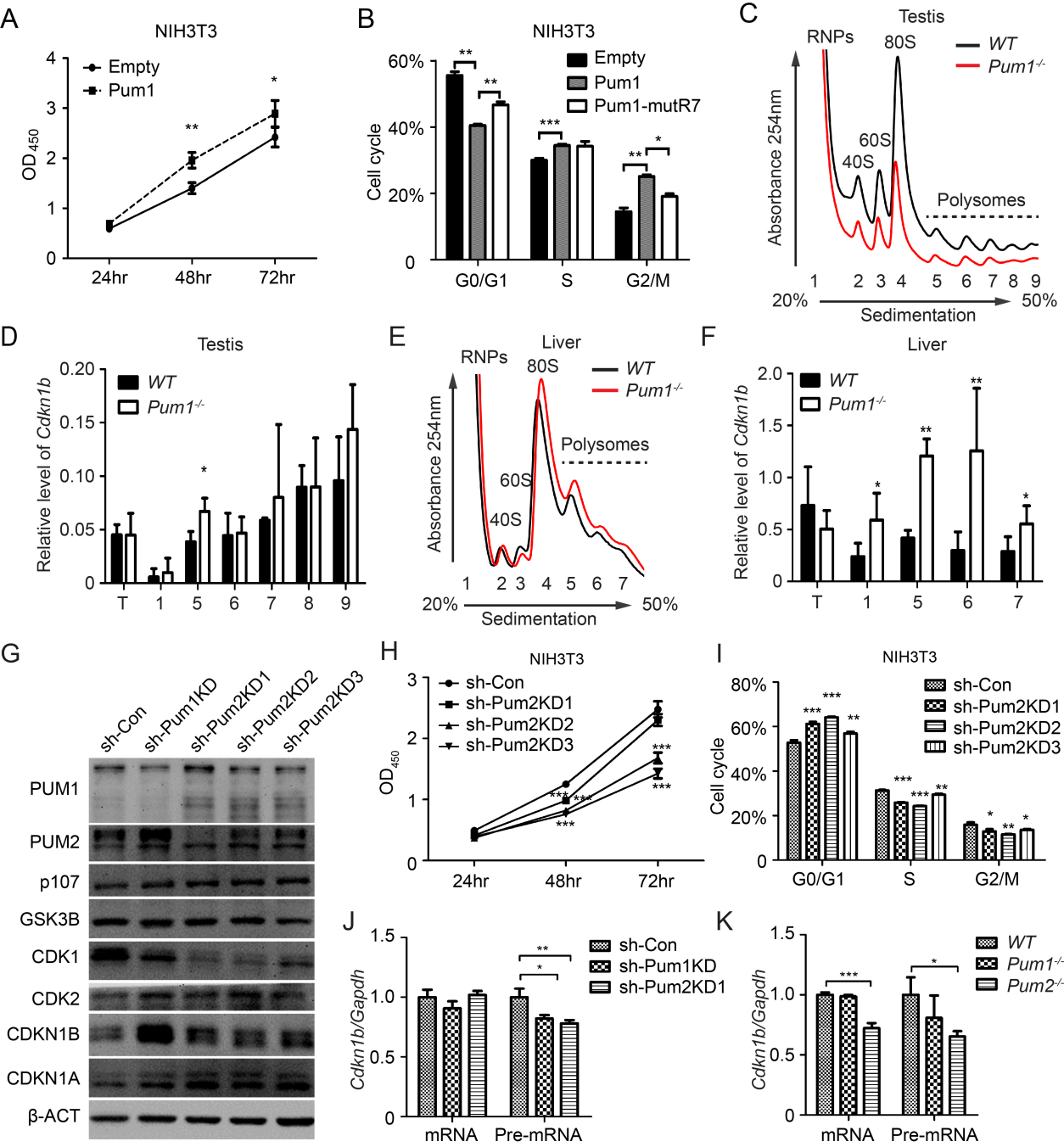
A
NIH3T3
Empty
Pum1
OD450
24hr
48hr
72hr
B
NIH3T3
Empty
Pum1
Pum1-mutR7
Cell cycle
G0/G1
S
G2/M
C
Testis
RNPs
80S
60S
40S
WT
Pum1-/-
Absorbance 254nm
Polysomes
Sedimentation
20%
50%
D
Testis
WT
Pum1-/-
Relative level of Cdkn1b
E
Liver
RNPs
80S
60S
40S
WT
Pum1-/-
Absorbance 254nm
Polysomes
Sedimentation
F
Liver
WT
Pum1-/-
Relative level of Cdkn1b
G
sh-Con
sh-Pum1KD
sh-Pum2KD1
sh-Pum2KD2
sh-Pum2KD3
PUM1
PUM2
p107
GSK3B
CDK1
CDK2
CDKN1B
CDKN1A
β-ACT
H
NIH3T3
sh-Con
sh-Pum2KD1
sh-Pum2KD2
sh-Pum2KD3
OD450
24hr
48hr
72hr
I
NIH3T3
sh-Con
sh-Pum2KD1
sh-Pum2KD2
sh-Pum2KD3
Cell cycle
G0/G1
S
G2/M
J
sh-Con
sh-Pum1KD
sh-Pum2KD1
Cdkn1b/Gapdh
mRNA
Pre-mRNA
K
WT
Pum1-/-
Pum2-/-
Cdkn1b/Gapdh
mRNA
Pre-mRNA

Figure S5. Cell growth and cell cycle analyses of *Pum1* mutant cells, *Pum1* overexpressing cells and *Pum2* knockdown cells, Related to Figure 4.

(A) Cell proliferation assay of NIH3T3 cell lines overexpressing mouse *Pum1* (m*Pum1*) and empty vector (Empty) by CCK8 assay.

(B) Cell cycle analyses on NIH 3T3 cells overexpressing wild type m*Pum1*, showed significantly decreased G0/G1 phase cells.

(C-F) *Cdkn1b* mRNA were also enriched in one or more polysome fractions from testes (C, E) or from liver (D, F) while total RNA (T) were not different. Tissue lysate from $Pum1^{+/+}$ (3) and $Pum1^{-/-}$ (3) mice were used. Peak position of free RNP (1), 40S (2), 60S (3) and 80S ribosome (4) and polysomes (5,6,7,8,9) are indicated. Wild type (black line) and $Pum1^{-/-}$ mutant (red line) profiles were over-layed. The values were normalized against β-Actin. The experiments were performed in triplicate.

(G) Western blot analysis of Cdkn1b and other cell cycle protein levels in *Pum1* knockdown or *Pum2* knockdown NIH 3T3 cells.

(H) Cell proliferation detected by CCK8 in *Pum2* knockdown (sh-Pum2KD1, sh-Pum2KD2, sh-Pum2KD3) and control (sh-Con) NIH 3T3 cells.

(I) Cell cycle detection of *Pum2* knockdown and control NIH 3T3 cells.

(J and K) Expression levels of precursor mRNA (pre-mRNA) and mature mRNA were determined by qRT-PCR in NIH3T3(J) and MEF(K) cells depleted for either *Pum1* or *Pum2*.

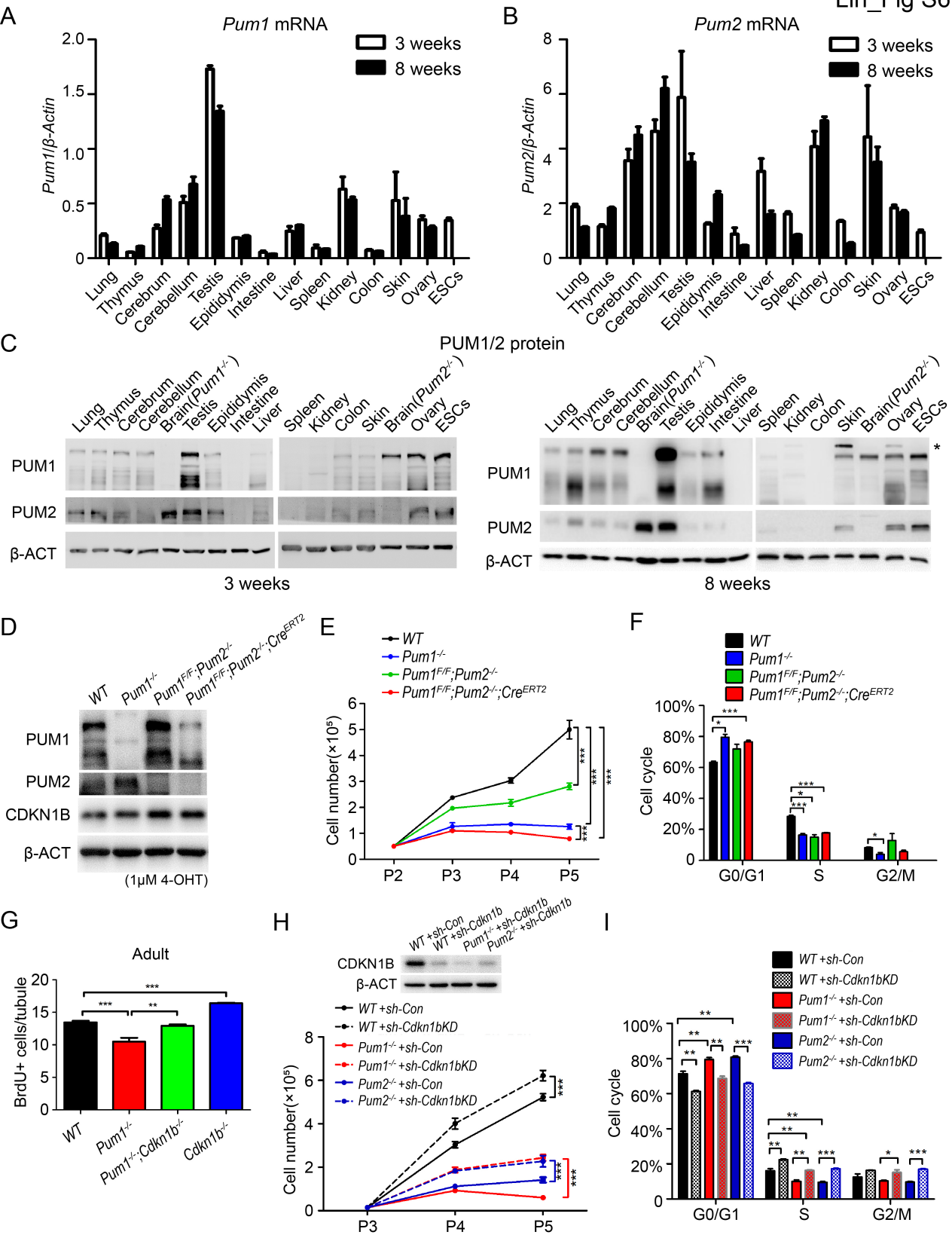
A
Pum1 mRNA
3 weeks
8 weeks
Pum1/β-Actin
2.0
1.5
1.0
0.5
0
Lung
Thymus
Cerebrum
Cerebellum
Testis
Epididymis
Intestine
Liver
Spleen
Kidney
Colon
Skin
Ovary
ESCs
B
Pum2 mRNA
3 weeks
8 weeks
Pum2/β-Actin
8
6
4
2
0
C
PUM1/2 protein
Brain(Pum1-/-)
Brain(Pum2-/-)
PUM1
PUM2
β-ACT
3 weeks
8 weeks
*
D
WT
Pum1-/-
Pum1F/F;Pum2-/-
Pum1F/F;Pum2-/-;CreERT2
PUM1
PUM2
CDKN1B
β-ACT
(1μM 4-OHT)
E
WT
Pum1-/-
Pum1F/F;Pum2-/-
Pum1F/F;Pum2-/-;CreERT2
Cell number(×10⁵)
6
5
4
3
2
1
0
P2
P3
P4
P5
***
F
WT
Pum1-/-
Pum1F/F;Pum2-/-
Pum1F/F;Pum2-/-;CreERT2
Cell cycle
100%
80%
60%
40%
20%
0
G0/G1
S
G2/M
*
***
G
Adult
BrdU+ cells/tubule
20
15
10
5
0
***
**
WT
Pum1-/-
Pum1-/-;Cdkn1b-/-
Cdkn1b-/-
H
WT +sh-Con
WT +sh-Cdkn1b
Pum1-/- +sh-Cdkn1b
Pum2-/- +sh-Cdkn1b
CDKN1B
β-ACT
WT +sh-Con
WT +sh-Cdkn1bKD
Pum1-/- +sh-Con
Pum1-/- +sh-Cdkn1bKD
Pum2-/- +sh-Con
Pum2-/- +sh-Cdkn1bKD
Cell number(×10⁵)
8
6
4
2
0
P3
P4
P5
***
I
WT +sh-Con
WT +sh-Cdkn1bKD
Pum1-/- +sh-Con
Pum1-/- +sh-Cdkn1bKD
Pum2-/- +sh-Con
Pum2-/- +sh-Cdkn1bKD
Cell cycle
100%
80%
60%
40%
20%
0
G0/G1
S
G2/M
**
*
***

Figure S6. Similar tissue expression profiles of *Pum1* and *Pum2* and their roles in the regulation of cell proliferation and cell cycle via *Cdkn1b*, Related to Figure 7.

(A and B) qRT-PCR analysis of *Pum1* (A) and *Pum2* (B) mRNA levels in different tissues of 3-week-old and adult wild-type mice, normalized to β-Actin. Error bars indicate standard deviation.

(C) Western blot analyses of protein levels of PUM1 and PUM2 in different tissues of 3-week-old and adult mice. * non-specific bands. ESC—embryonic stem cells.

(D) Western blot result showed the expression levels of PUM1 and PUM2 in *WT*, *Pum1*$^{-/-}$, *Pum1*$^{F/F}$ *Pum2*$^{-/-}$ and *Pum1*$^{F/F}$ *Pum2*$^{-/-}$ *Rosa*^{ERT2Cre} MEF cells by 4-hydroxytamoxifen (4-OHT, 1uM).

(E) Growth difference among the MEFs of the different genotypes from passage 2 to 5 (P2 to P5).

(F) Cell cycle distribution of the MEFs was assessed by PI staining and FACS analysis.

(G) Cell proliferation was analyzed by counting the BrdU positive cells in adult testis sections of *WT*, *Pum1*$^{-/-}$, *Pum1*$^{-/-}$*;Cdkn1b*$^{-/-}$ and *Cdkn1b*$^{-/-}$ genotypes.

(H) Western blot result shows that knockdown *Cdkn1b* in *WT*, *Pum1*$^{-/-}$ and *Pum2*$^{-/-}$ MEF cells and MEF cells growth curve were detected from passage 3 to 5 (P3-P5).

(I) Cell cycle distribution of MEF cells were assessed by PI staining and FACS analysis.

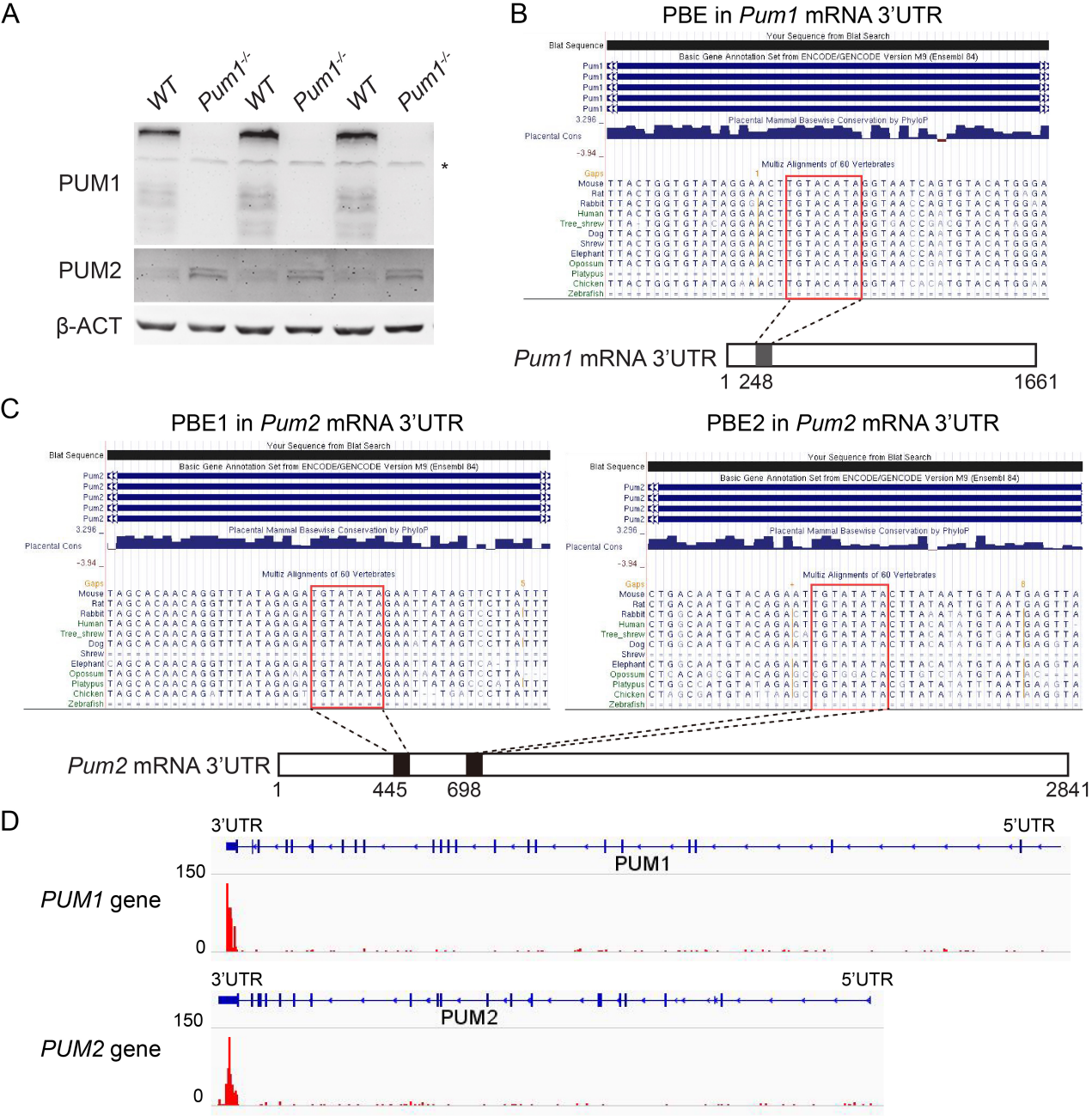
A
WT
Pum1-/-
WT
Pum1-/-
WT
Pum1-/-
PUM1
PUM2
β-ACT
*
B
PBE in Pum1 mRNA 3'UTR
Your Sequence from Blat Search
Blat Sequence
Basic Gene Annotation Set from ENCODE/GENCODE Version M9 (Ensembl 84)
Placental Mammal Basewise Conservation by PhyloP
Placental Cons
Multiz Alignments of 60 Vertebrates
Mouse
Rat
Rabbit
Human
Tree_shrew
Dog
Shrew
Elephant
Opossum
Platypus
Chicken
Zebrafish
Pum1 mRNA 3'UTR
1
248
1661
C
PBE1 in Pum2 mRNA 3'UTR
PBE2 in Pum2 mRNA 3'UTR
Pum2 mRNA 3'UTR
1
445
698
2841
D
3'UTR
5'UTR
PUM1
PUM2
PUM1 gene
PUM2 gene
150
0

Figure S7. Increased PUM2 tissue expression in absence of *Pum1* and conserved Pumilio-binding element (PBE) in 3' UTR of *Pum1* and *Pum2* genes, Related to Figure 7.

(A) Western blot analysis showed increased protein levels of *Pum2* in adult *Pum1*$^{-/-}$ testes compared with wild type.

(B and C) Highly conserved PBE motifs in the 3' UTRs of *Pum1* (B), and *Pum2* (C), suggesting functional importance of PBEs.

(D) Read density track along human PUM1 and PUM2 from eCLIP data on human PUM2 revealed significant enrichment of binding sites at 3'UTR of *PUM1* and *PUM2.*

Table S1. List of primers used in this study, Related to STAR Methods,

Related to STAR Methods.

Primer	**Sequence (5'-3')**	**Use**
Pum1 forward	GCAGCTACAAACTCTGCTACTC	qRT-PCR
Pum1 reverse	CAAGACTGGATAACCTGGCATAC	qRT-PCR
Pum2 forward	GCAGGTCAGCGTCCTATTACTC	qRT-PCR
Pum2 reverse	CTTGTGCTGCTGTTGAACTTATTA	qRT-PCR
Cdkn1b forward	AGCTTGCCCGAGTTCTACTA	qRT-PCR
Cdkn1b reverse	CTTCTGTTCTGTTGGCCCTT	qRT-PCR
β-*Actin* forward	TGACCCAGATCATGTTTGAG	qRT-PCR
β-*Actin* reverse	GAGTCCATCACAATGCCTG	qRT-PCR
Gapdh forward	ACCCAGAAGACTGTGGATGG	qRT-PCR
Gapdh reverse	GGTCCTCAGTGTAGCCCAAG	qRT-PCR
Cdkn1b exon forward	AGCTTGCCCGAGTTCTACTA	qRT-PCR
Cdkn1b exon reverse	CTTCTGTTCTGTTGGCCCTT	qRT-PCR
Cdkn1b intron forward	CCAAAGGATAGGGACGGTCG	qRT-PCR
Cdkn1b intron reverse	CGAACCTCTGGGAAATGGGTT	qRT-PCR
KOF1-P1	CATGAGTTTGGGAGGCATTT	Genotyping
LOXGTR-P2	GTCTTGTGGCAACTAGGGTA	Genotyping
KOR1-P3	GTGGCTAACAACTGCTGCAA	Genotyping